Appl. Phys. B 59, 187–193 (1994)

Applied Physics B Lasers and Optics

Frequency measurement of $^{130}Te_2$ resonances near 467 nm

Ph. Courteille, L. S. Ma*, W. Neuhauser, R. Blatt

Institut für Laser-Physik, Universität Hamburg, Jungiusstrasse 9, D-20355 Hamburg, Germany
(Fax: +49-40/4123-6571)

Received 28 March 1994/Accepted 16 May 1994

Abstract. Precision spectroscopy on molecular tellurium is performed by measuring the frequency difference between the observed lines and an eigenfrequency of a high-finesse cavity mode. The mode frequency is derived from a measurement of the cavity's free spectral range taking into account the cavity dispersion due to phase shifts in the dielectric mirror coatings. The experimental technique is based on dual frequency modulation and is applied to determine the transition wavenumbers of several lines in $^{130}Te_2$ near 467 nm with an uncertainty of 2×10^{-8}.

PACS: 07.65.Eh, 33.80, 42.50

Precision spectroscopy on $^{130}Te_2$ with reference to iodine stabilized HeNe lasers has been performed by several research groups and proved successful in transferring the iodine wavelength standards to the $^{130}Te_2$ reference frequencies in the region for 471–502 nm and in particular near 486 nm [1–6]. More recently, reference lines near 467 nm have become of increasing interest [7]. This is due to the fact that significant efforts are currently taken to search and precisely measure an ultranarrow optical transition in single trapped Yb^+ ions at 467 nm which has been proposed as the basis for an optical frequency standard [8]. Since this transition frequency is only known with an uncertainty of about 50 MHz (8×10^{-8}), and its linewidth is expected to be on the order of a few Hz, very precise reference frequencies are required for the reproducible search of the transition.

In a recent experiment, we have employed Modulation Transfer Spectroscopy (MTS) to determine reference frequencies in $^{130}Te_2$ near 467 nm [7]. The accuracy in these earlier investigations was limited by the inaccuracy of the wavemeter which was about 200 MHz. More precise measurements either require a much improved instrument for measuring wavelength or transferring the precision of other well known resonances to the unknown wavelengths region. In the experiment described below both techniques have been applied.

For a precision measurement of the wavenumbers we used a reference cavity with a precisely known FSR. The order number N of the resonant cavity mode can be determined without ambiguities using a simple wavemeter with 200 MHz resolution if the uncertainty of the FSR is less than $\Delta\nu = \nu/N$ (where ν is the FSR and N the order number of the cavity modes) and when residual phase shifts introduced by the dielectric mirrors are known. With the cavity used in this experiment the FSR has to be determined with an uncertainty smaller than 1 kHz. A rough value of the FSR is usually obtained by measuring the length of the cavity spacer. More accurate values of the FSR may be derived from a precisely known transition frequency of a molecular line [9], or by measuring the beat frequency between two tunable lasers locked to different cavity modes [10]. This can be achieved by locking sidebands generated by means of Electro-Optic Modulators (EOM) to adjacent cavity modes [11]. For our measurement we employ a technique based on Dual-Frequency Modulation (DFM) being similar to that reported in [12], but with the use of only one EOM and a supercavity which is kept at a fixed frequency. Thus we obtain, (i) precise frequency control within two adjacent cavity modes and, (ii) a narrowed laser bandwidth by referencing the output frequency to the cavity without influencing the active laser (post-stabilization).

With the techniques discribed below we are able to derive the value of the FSR with a statistical uncertainty of about 15 Hz. Thus, the optical frequency can be determined with an uncertainty of about 13 MHz at any detuning in the range 462–472 nm. As an experimental test we compare our results for the transition frequency of a line in $^{130}Te_2$ near 471 nm with a previously determined value [1] which is known with an uncertainty of 1.4 MHz (2.2×10^{-9}) and find agreement within our error limits. At the current level of precision residual phase

* *Permanent address:* Department of Physics, East China Normal University, Shanghai 200062, People's Rep. China

shifts in the dielectric coatings do not significantly deteriorate the results.

The paper is organized as follows. Section 1 comprises the general idea of the experiment and the experimental setup. Details on the measurement of the FSR, the phase shifts due to the dielectric mirrors and the residual uncertainties are given in Sect. 2 and the spectroscopic results for the measured $^{130}Te_2$ lines are presented in Sect. 3. Section 4 concludes with a brief summary.

1 Detuning unit and post-stabilization

A laser beam of frequency ω near 467 nm is modulated by means of a wideband EOM which serves as an optical phase modulator and which is driven at a frequency Ω thus generating sidebands at $\omega \pm n \cdot \Omega$. When one of the optical sidebands is locked to an eigenfrequency of a cavity the frequency of the carrier can be tuned just by varying the frequency Ω. In order to employ the Pound-Drever technique [14] to lock the laser on the optical sideband additional sidebands are required, which give rise to the well known dispersion signal when reflected from the cavity and when the laser frequency is tuned across the eigenfrequency of the cavity. This could be achieved by means of a second EOM placed in the laser beam [12, 13]. A simpler method, however, consists in applying frequency modulation by δ to the modulation frequency Ω, thus creating additional sidebands at $\omega + \Omega \pm \delta$ and $\omega - \Omega \pm \delta$. This results in a spectrum consisting of a carrier with two groups of sidebands which is shown in the lower part of Fig. 1a. The resulting power spectrum of the laser beam is shown in Fig. 1b, where a spectral recording of the transmitted light of a Fabry-Perot interferometer is shown. Note that in this example the sideband groups can be observed close to the carrier frequency: At a cavity mode N the left group represents the upper sidebands pertaining to the cavity mode $N-1$ and the right group shows the lower sidebands corresponding to the cavity mode $N+1$ as indicated in the upper trace of Fig. 1a.

A detailed scheme of the experimental setup is shown in Fig. 2. The output of the dye laser passes a $\lambda/2$ wave plate and is then split in two parts by beamsplitter BS1. Part of the beam passes the beam splitter and is used for (pre-) stabilization of the laser frequency by means of the Pound-Drever method [14]. Thus, the emission frequency shows narrowed bandwidth and is characterized in terms of the square root of its Allan-variance which has been measured to be $\sigma(\tau) = 7 \times 10^{-16}\ \tau^{-\frac{1}{2}}\ \mathrm{Hz}^{\frac{1}{2}}$ for time periods between 10^{-5} s and 1 s [15]. This represents the laser instability with respect to the cavity used in the Pound-Drever stabilizer. The absolute laser frequency is more uncertain due to fluctuations of the cavity length used for pre-stabilization.

The reflected part of the laser beam at beamsplitter BS1 passes a $\lambda/4$ wave plate and an AOM which serves to shift the laser frequency and is used for scanning the frequency. In addition, the AOM prevents optical feedback from the interferometer. Subsequently the laser beam is split again in a beam which is fed to the experiment and the wavemeter setup and another beam which is used for the DFM technique. The latter beam passes a wideband EOM which is driven by an rf synthesizer at frequency $\Omega/2\pi = 0.01 - 1$ GHz. The synthesizer itself has an external Frequency Modulation (FM) option, and Ω is modulated with the radiofrequency $\delta/2\pi = 700$ kHz. This modulation results in the power spectrum as shown in Fig. 1a.

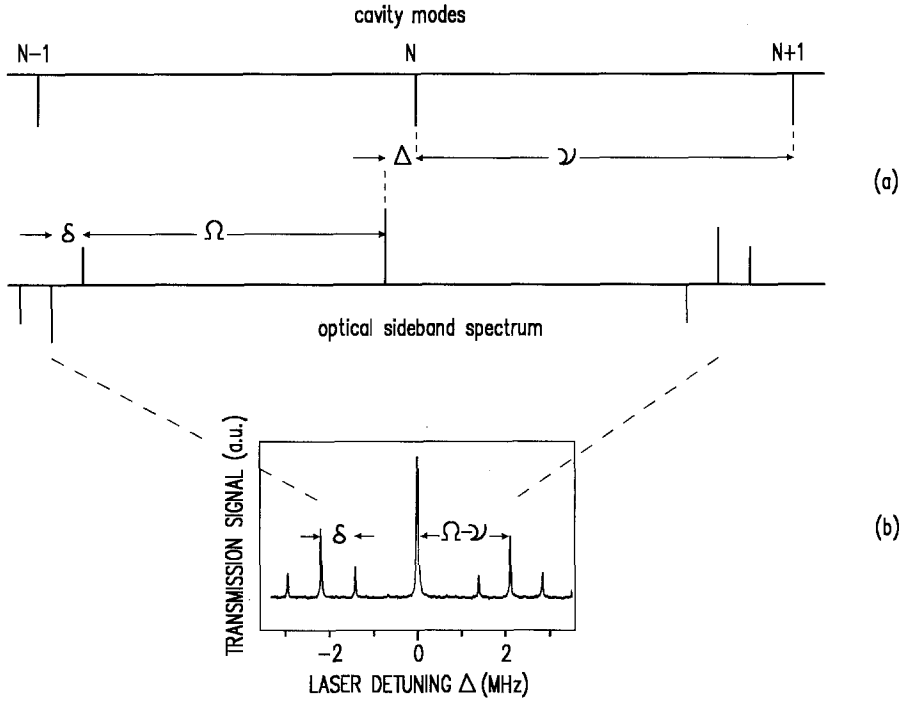

Fig. 1. (**a**) Cavity modes and spectrum of the optical sidebands with double FM. ν is the mode spacing, Ω is the modulation frequency for the optical sidebands, δ denotes the rf modulation frequency, Δ is the detuning between the carrier and a cavity resonance frequency. (**b**) Transmission spectrum from a Fabry-Perot interferometer, recorded while detuning the laser frequency Δ. Note that when $\Omega \approx \nu$ both sideband triplets can be observed close to the carrier frequency

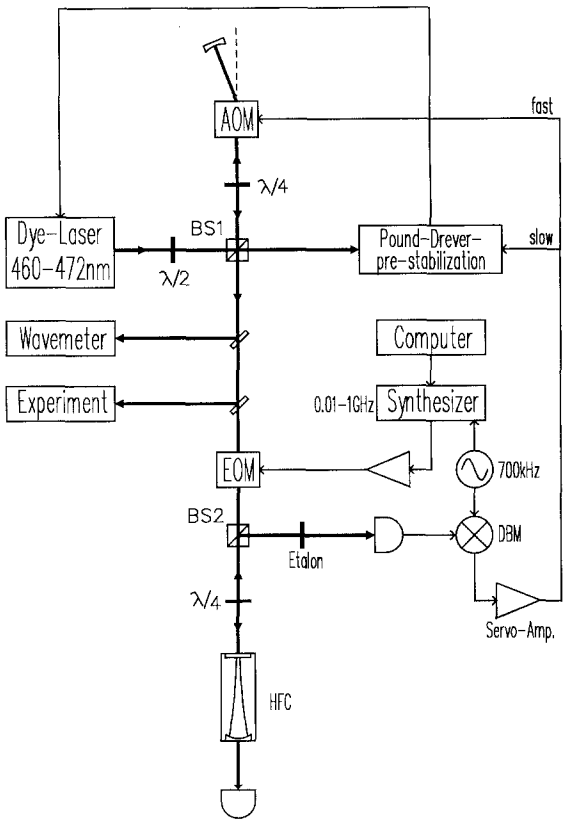

Fig. 2. Experimental scheme of the post-stabilization. BS1, BS2: Polarizing Beam Splitters, HFC: High Finesse Cavity ($F=36000$), DBM: Double Balanced Mixer, AOM: Acousto-Optic Modulator, EOM: Electro-Optic Modulator. The reference cavity of the Pound-Drever-prestabilization is tunable

The modulated beam is then matched to an optical cavity placed in a high vacuum chamber and temperature stabilized to better than 0.01° C. The ZERODUR spacer of this cavity is 200.7 mm long corresponding to a FSR of 747 MHz. The cavity consists of a plane mirror and a mirror with 500 mm radius of curvature, the dielectric coatings yield the finesse 36000. The reflected beam is focussed on a photodiode, and the photo current is demodulated with frequency δ. When the dispersive slope of the demodulated signal is used to lock the laser to one of the optical sidebands, the slow components (below 1 Hz) of the error signal are fed to the PZT of the tunable reference cavity of the pre-stabilized laser, and the fast components (above 1 Hz to 40 kHz) are fed to an AOM. In this way the output frequency of the laser is referred to the stable high finesse cavity (post-stabilization).

2 Absolute frequency measurement

Since the laser can be detuned with respect to a cavity mode with radio frequency precision, for an absolute frequency measurement it is sufficient to precisely measure the frequency of an adjacent cavity mode. If the FSR of the cavity is known with high precision, this problem is solved just by determining the order number N of the cavity mode and by taking into account possible phase shifts in the dielectric coatings of the mirrors. The mode order can be read directly without ambiguity from a wavemeter with low resolution, if the FSR is known with better accuracy than $\Delta\nu = \nu/N$ (were ν is the FSR). With the cavity used in this experiment the accuracy has to be better than 1 kHz.

The FSR of the reference cavity is determined in the following way. The separation Ω of the sidebands generated by the electro-optic modulator from the laser (carrier) frequency is made to match the FSR. Then, both the carrier and the sidebands suffer the same phase shift and amplitude attenuation upon reflection from the cavity at any laser detuning around the cavity mode. Thus, beating the carrier with both sidebands in the reflected light generates a pair of beat notes at the photodiode with the same amplitude but opposite phases, and hence the recorded signal vanishes. When the separation between sidebands and carrier does not match the FSR, the beat notes are unbalanced, and the reflected signal does not vanish.

In order to avoid detection of the reflected signal directly at the high frequency $\Omega/2\pi = 747$ MHz, the modulation frequency Ω is in turn modulated with the radio-frequency $\delta/2\pi = 700$ kHz, and the reflected signal is demodulated at δ. The sideband spectrum is derived from the expansion of the electric field $\exp[i\omega t + i\beta \sin(\Omega t + \alpha \sin \delta t)]$ in terms of Bessel functions, where ω denotes the carrier frequency, β is the depth of the modulation at frequency Ω, and α is the depth of modulation at frequency δ. Considering only first-order sidebands we find:

$$
\begin{aligned}
&e^{i[\omega t + \beta \sin(\Omega t + \alpha \sin \delta t)]} \\
&= e^{i\omega t}[-\mathfrak{J}_1(\beta)\, e^{-i(\Omega t + \alpha \sin \delta t)} + \mathfrak{J}_0(\beta) + \mathfrak{J}_1(\beta)\, e^{i(\Omega t + \alpha \sin \delta t)}] \\
&= e^{i\omega t}[-\mathfrak{J}_1(\beta)\,\mathfrak{J}_1(\alpha)\, e^{i(-\Omega-\delta)t} - \mathfrak{J}_1(\beta)\,\mathfrak{J}_0(\alpha)\, e^{-i\Omega t} \\
&\quad + \mathfrak{J}_1(\beta)\,\mathfrak{J}_1(\alpha)\, e^{i(-\Omega+\delta)t} + \mathfrak{J}_0(\beta) - \mathfrak{J}_1(\beta)\,\mathfrak{J}_1(\alpha)\, e^{i(\Omega-\delta)t} \\
&\quad + \mathfrak{J}_1(\beta)\,\mathfrak{J}_0(\alpha)\, e^{i\Omega t} + \mathfrak{J}_1(\beta)\,\mathfrak{J}_1(\alpha)\, e^{i(\Omega+\delta)t}],
\end{aligned}
\tag{1}
$$

where $\mathfrak{J}_k(x)$ is the Bessel function of the order k. As shown in Fig. 1a, the spectrum of the modulated laser beam consists of the carrier at frequency ω and two groups of optical sidebands at $\omega \pm \Omega$ which in turn show symmetric rf sidebands at $\omega \pm \Omega \pm \delta$. For a frequency Ω of the same order of magnitude as the free spectral range ν but much larger than frequency δ, the carrier ω interacts with the cavity mode ω_0. The group of sidebands located at $\omega - \Omega \pm \delta$ only interacts with the cavity mode $\omega_0 - \nu$ and the group of sidebands at $\omega + \Omega \pm \delta$ is resonant with the cavity mode $\omega + \nu$.

The reflection response of a resonator to a light field E_0 is given by [16, 17]:

$$
E_r(\omega) = E_0 \sqrt{R}\, \frac{1 - e^{-2\pi i\, \omega/\nu}}{1 - R\, e^{-2\pi i\, \omega/\nu}}, \tag{2}
$$

where R is the reflectivity of the mirrors, and ν is the free spectral range of the cavity. Attenuation and phase shift of the reflected light field are easily calculated from $E_r(\omega) = |E_r(\omega)| \exp[i\varphi(\omega)]$. When we insert (2) into (1)

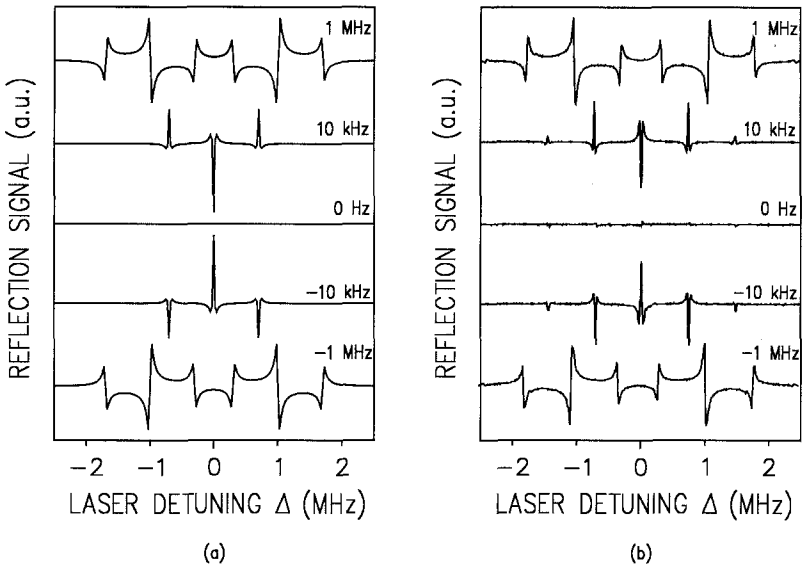

Fig. 3. a Calculation of the lineshape of the demodulated reflexion signal via the laser detuning Δ with various offsets between the modulation frequency Ω and the FSR ν: $(\Omega-\nu)/2\pi = -1$ MHz, -10 kHz, 0 Hz, 10 kHz, and 1 MHz. **b** Measurement of the lineshape of the demodulated reflexion signal for the same offset frequencies as in (a)

we obtain the sideband spectrum of the reflected light dependent on the laser frequency ω, the modulation frequency Ω and the reflectivity R of the cavity mirrors. The beat note at the photodiode is proportional to $E_r(\omega)\,E_r^*(\omega)$ and is demodulated with $\exp(-i\delta t)$. Thus, the signal is given by

$$I_r = I_0 \mathfrak{I}_1(\beta)^2\,\mathfrak{I}_0(\alpha)\,\mathfrak{I}_1(\alpha)\,\mathrm{Re}[+E_r^*(\omega+\Omega)\,E_r(\omega+\Omega+\delta) - E_r^*(\omega-\Omega)\,E_r(\omega-\Omega+\delta) - E_r(\omega+\Omega)\,E_r^*(\omega+\Omega-\delta) + E_r(\omega-\Omega)\,E_r^*(\omega-\Omega-\delta). \quad (3)$$

Equation (3) can be interpreted in the following way. Each of the four contributions to the signal arises from the beating between one of the optical sidebands $E_r(\omega\pm\Omega)$ with its rf sub-sidebands $E_r(\omega\pm\Omega\pm\delta)$. Considering $E_r(\omega\pm\nu)=E_r(\omega)$ and the modulation frequency $\Omega=\nu$, the first and second term compensate and also compensation occurs between the third and fourth term. Thus, the signal can be minimized via the modulation frequency Ω, and by this means it is possible to measure the FSR directly. Fig. 3a visualizes (3) and shows the signal as a function of the detuning for different frequency offsets between the modulation frequency Ω and the free spectral range ν. It is clearly seen that the signal diminishes with decreasing $\Omega-\nu$. Inspection of (3) reveals that the contrast of the signal can be maximized by setting the modulation indices to $\alpha\approx 1.1$ and $\beta\approx 1.84$.

Figure 3b shows the measured lineshape of the reflected signal for different offset frequencies between the modulation frequency Ω and the free spectral range ν. At the laser wavelength 466.751 nm the smallest signal amplitude was found at $\Omega/2\pi = 747040953$ (15) Hz, and therefore we identify this value with our FSR. The signals were taken with a time constant of 100 ms. For an offset frequency $\Omega-\nu = 2\pi\,100$ Hz we obtain a signal-to-noise ratio of about 10.

An important problem in the measurements is the residual Amplitude Modulation (AM) produced by the EOM, which results in asymmetric amplitudes of the optical sidebands and is present both at frequency Ω and δ. In both cases, the detector signal created by the sidebands that are reflected from the cavity does not vanish completely when the carrier is on resonance. The asymmetric character of the line profile may introduce a systematic error in the determination of the FSR. Experimentally, we balanced the amplitude of the sidebands by placing an etalon just in front of the detector. A 0.5 mm thick etalon with a finesse of 2.6 is used in our experiment and could reduce the unwanted asymmetries due to residual AM to be about 7% of the FM amplitude.

In addition the resolution of our apparatus is limited by frequency jitter of the prestabilized laser and the instability of the mode frequency of the reference cavity used for post-stabilization. We found both to be on the same order of magnitude as the cavity linewidth, i.e., 20 kHz, mainly due to acoustic noise which blurs the reflection signal. This is actually the main limitation of the precision of our measurement rather than the signal-to-noise ratio.

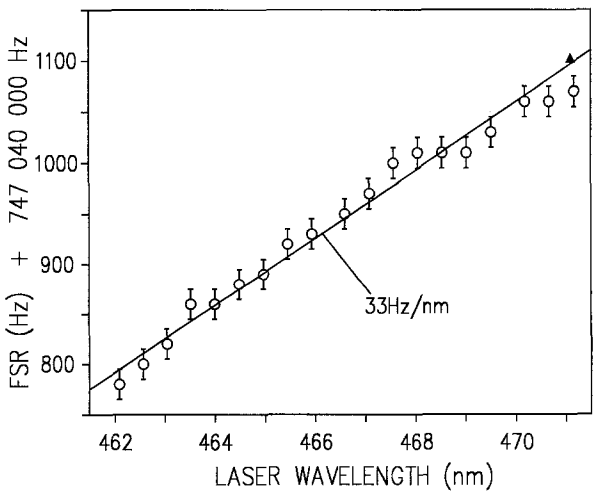

Fig. 4. Dispersion of the FSR. The value for the FSR changes with 33 (9) Hz/nm. The filled triangle shows the value for the FSR obtained from a calibration using the frequency of the line found at NIST [1] near 21221.012274 cm^{-1}

The light reflected from a dielectric mirror is subject to phase shifts which depend on the coating and on the wavelength of the light. Therefore the value v of the FSR of the cavity depends on the wavelength at which a measurement is taken, and the dispersion has to be taken into account when the cavity is used at eigenfrequencies spread over a wide range [18]. Phase shifts in cavities have been observed experimentally [10, 18, 19]. The mirrors used in our setup are identical with those used in [10]. In this experiment the authors measured a dispersion of the FSR of about 1.3 Hz/nm near 486 nm. Since the 467 nm wavelength is near the edge of the high reflective coating the phase shift was found to be much larger in our case. Figure 4 shows the measured FSR at different laser wavelengths. The dispersion is linear in the wavelength region of interest so that we can fit a straight line with a slope of 33 (9) Hz/nm between 462 nm and 472 nm.

3 Reference lines in $^{130}Te_2$

The accuracy of our spectrometer can be verified and utilized doing spectroscopy on molecular transition lines in $^{130}Te_2$, employing the method of Doppler-free MTS as discribed in [7]. The experimental configuration is shown in Fig. 5. The post-stabilized laser beam passes a $\lambda/2$ wave plate and is then divided into pump beam and probe beam by the polarizing beam splitter BS3. The optical phase modulator is driven by an rf amplifier at 6 MHz and generates sidebands on the pump beam. Pump and probe beam counterpropagate through the $^{130}Te_2$ cell. The initially unmodulated probe beam carries the MTS signals and is directed on a photodiode where an optical heterodyne current signal is produced. The MTS signals are extracted from this signal by a double-balanced mixer and recorded by an Analog-Digital-Converter (ADC).

As soon as a $^{130}Te_2$ resonance has been identified with the help of a wavemeter, the order N of an adjacent cavity mode is determined from the wavemeter measurement since the FSR and the corresponding phase shifts are well known. Then, one of the optical sidebands produced by the EOM is locked to the cavity mode, while the carrier is tuned to the $^{130}Te_2$ line, so that the frequency gap Δ_{gap} between the $^{130}Te_2$ line and the adjacent cavity mode is known with radiofrequency precision. The transition wavenumber of the $^{130}Te_2$ line can now be determined from $k = (Nv/2\pi + \Delta_{gap})/c$, where c is the speed of light.

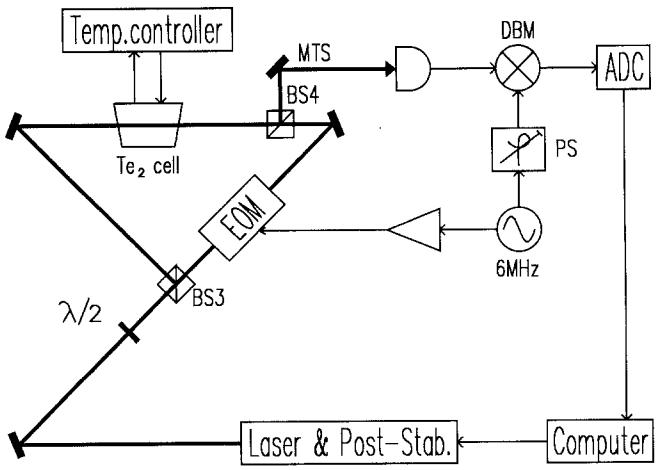

Fig. 5. Experimental setup for MTS on $^{130}Te_2$. BS3, BS4: Polarizing Beam Splitters, EOM: Electro-Optic Modulator, DBM: Double Balanced Mixer, ADC: Analog-Digital-Converter, PS: Phase Shifter

Gillaspy and Sansonetti at NIST [1] recently presented new reference lines of $^{130}Te_2$ in the 471–502 nm wavelength range with 44×10^{-6} cm^{-1} (1.4 MHz) accuracy. The line closest to our tuning range is at $k = 21221.012274$ (44) cm^{-1}. The cavity mode of the next-lower frequency was found to have the order $N = 851613$, and the frequency gap was measured to be $\Delta_{gap} = 28.0$ (1) MHz. From this measurement we obtain the transition frequency $k = 21221.01212$ (44) cm^{-1}.

The NIST measurements whose uncertainty is small could be exploited to determine the actual FSR v of the cavity more precisely. The filled triangle in Fig. 4 shows the FSR derived from the NIST measurements and agrees well with our measurements of the cavity dispersion. Transferring this precision to distant lines, however, requires improved knowledge of the cavity dispersion, so that this calibration currently cannot be used with our setup to determine the molecular transition frequencies near 467 nm.

In an earlier measurement [7], some transitions of $^{130}Te_2$ near 467 nm were found using MTS. Some of these lines can be identified with lines listed in the tellurium atlas [20], but most of them have not been measured so far. The accuracy of the labelled lines is given to be 0.002 cm^{-1} (60 MHz), and the frequency of the unlisted lines was measured by means of a wavemeter with an accuracy of 0.007 cm^{-7} (200 MHz). The particular $^{130}Te_2$ line which is near the resonance frequency of the $^2F_{7/2} - {}^2S_{1/2}$ octupole transition in Yb^+ is at $k = 21418.702$ (2) cm^{-1} [7]. The frequency gap between the reference line k and the nearest cavity mode was measured to be $\Delta_{gap} = 360.7$ (1) MHz, and the cavity mode order was found to be $N = 859546$. This gives an improved value for the wavenumber $k = 21418.69838$ (44) cm^{-1}.

In order to check the reproducibility, the measurements were repeated during several days. The day-to-day standard deviation of the measured frequency gap Δ_{gap} was found to be within 10 MHz due to thermal drifts of the cavity spacing, and thus it is of the same order of magnitude as the statistical uncertainty resulting from the FSR measurement (13 MHz). However, since the measurement is carried out very fast (a measurement of the FSR and the laser frequency takes a few minutes), these long term drifts do not affect the accuracy of our measurement.

Minor contributions to the total uncertainty result from the tellurium cell. In [6] the day-to-day reproducibility was found to be on the order of 0.2 MHz, and the cell-to-cell variation was observed to be 0.4 MHz. These uncertainties are much smaller than our accuracy and need not to be taken into account. The mean measured

Table 1. Measured wavenumber for some $^{130}Te_2$ lines near 467 nm. The first column shows the value found in [1] having a standard deviation of 44×10^{-6} cm^{-1} and [20] having a standard deviation of 20×10^{-4} cm^{-1}. The second column presents the measured wavenumber using the value for the FSR $\nu/2\pi = 747040953$ (15) Hz and the mode order number N. The third column shows the difference of the values listed in the previous columns. The wavenumber marked "R" is used in the search of the octupole transition (cf. Fig. 6). Note that for the last wavenumber (near 471 nm) we used the FSR $\nu/2\pi = 747041103$ (15) Hz taking into account the measured cavity dispersion (cf. Fig. 4)

Wavenumber k from atlas and NIST [cm^{-1}]	Calibrated wavenumber k [cm^{-1}]	Difference	
		[cm^{-1}]	[MHz]
21420.5018 (20)	21420.50182 (44)	–	–
	21419.89012 (44)		
	21419.73045 (44)		
21419.3994 (20)	21419.39942 (44)	–	–
	21419.39824 (44)		
21419.2416 (20)	21419.28569 (44)	−0.0441	−1322
	21419.14823 (44)		
21419.0668 (20)	21419.07221 (44)	−0.0054	−162
	21419.04957 (44)		
21418.9438 (20)	21418.93976 (44)	+0.0040	+121
R:	21418.69838 (44)		
	21417.82654 (44)		
21417.7741 (20)	21417.77893 (44)	−0.0048	−145
	21417.39377 (44)		
21417.2920 (20)	21417.29082 (44)	+0.0012	+35
21416.8054 (20)	21417.80213 (44)	+0.0033	+98
	21221.08579 (44)		
21221.012274 (44)	21221.01212 (44)	+0.00015	+4.6

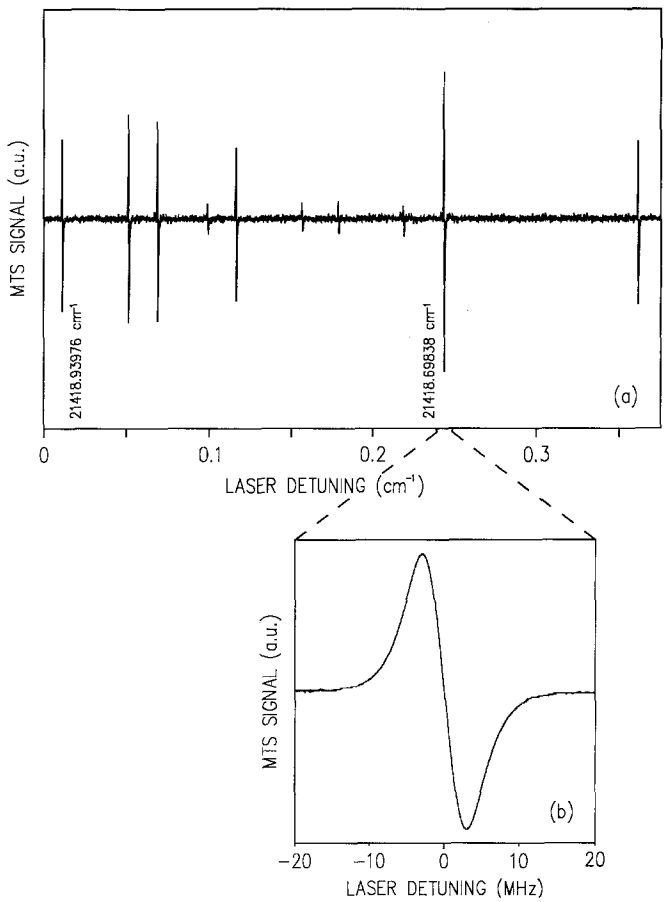

Fig. 6. a Tellurium spectrum near 467 nm. The labelled lines have been measured using the DFMT discribed in the text. **b** MTS signal of the reference line near 21418.69838 cm^{-1}. The signal-to-noise ratio is about 1000 with a time constant of 100 ms and a laser power of 2 mW

values for some lines in the vicinity of 467 nm are shown in Table 1. For several lines the atlas wavenumbers differ significantly from the wavenumbers found in this work. The uncertainty of the atlas wavenumbers probably occurs because many of the Doppler-limited lines observed by Fourier spectroscopy are not resolved but represent several molecular lines.

Figure 6a shows the tellurium spectrum near 467 nm. The lines have been measured with an accuracy of 13 MHz. The MTS signal of the reference line near 21418.69838 cm^{-1} is shown in Fig. 6b. The signal-to-noise ratio is about 1000 obtained with a time constant of 100 ms and a laser power of 2 mW; the total measurement time was about 2 min. Note that the center frequency of the line could be determined with a relative uncertainty of several 10 kHz.

4 Discussion

In summary, reference frequencies in $^{130}Te_2$ near 467 nm have been measured using a DFM technique. This technique turned out to be a convenient method for a measurement of the FSR, and for precision laser spectroscopy. There is no necessity to scan the laser frequency over a large tuning range doing fringe counting and making the laser frequency alternate between a reference laser and the wavelength to be measured. Therefore, the total measurement can be performed within a short period of time and thus the measurement uncertainties due to the long-term stability of the apparatus and the optical system can be reduced significantly. Further improvement, i.e., reduced residual AM and particularly an improved acoustical isolation of the laser and the re-

ference cavity would result in at least 10-fold better precision, thus yielding a simple spectrometer with absolute residual frequency uncertainty on the order of 1 MHz. Higher precision is even possible with a better knowledge of the phase shifts introduced by the dielectric mirror coatings.

In conclusion, a combined MTS setup for precision spectroscopy in $^{130}Te_2$ and using dual FM for the measurement of a cavity resonance ensures absolute reproducibility of the laser frequency within about 13 MHz. This is a necessary requirement for long time measurements such as the search for the very narrow octupole transition $^2F_{7/2} - {}^2S_{1/2}$ of Yb^+ ions.

Acknowledgements. We thank Prof. P.E. Toschek for continuous support and for providing the mirrors of the high finesse cavity. Ma Long-Sheng thanks the Universität Hamburg for hospitality during his stay as a guest scientist in 1992–1993. This work was supported by the Deutsche Forschungsgemeinschaft and the National Natural Science Fund of China.

References

1. J.D. Gillaspy, C.J. Sansonetti: J. Opt. Soc. Am. B**8**, 2414 (1991)
2. J.R.M. Barr, J.M. Girkin, A.I. Ferguson, G.P. Barwood, P. Gill, W.R.C. Rowley, R.C. Thompson: Opt. Commun. **54**, 217 (1985)
3. D.H. McIntyre, T.W. Hänsch: Phys. Rev. A **34**, 4504 (1986)
4. D.H. McIntyre, T.W. Hänsch: Phys. Rev. A **36**, 4115 (1987)
5. D.H. McIntyre, W.M. Fairbank Jr., S.A. Lee, T.W. Hänsch, E. Riis: Phys. Rev. A **41**, 4632 (1990)
6. G.R. Barwood, W.R.C. Rowley, P. Gill, J.L. Flowers, B.W. Petley: Phys. Rev. A **43**, 4783 (1991)
7. L.S. Ma, Ph. Courteille, G. Ritter, W. Neuhauser, R. Blatt: Appl. Phys. B **57**, 159 (1993)
8. R. Blatt, R. Casdorff, V. Enders, W. Neuhauser, P.E. Toschek: In *Proc. of Frequency Standards and Metrology*, ed. by A. De Marchi (Springer, Berlin, Heidelberg 1989) p. 306
9. J.E.M. Goldsmith, E.W. Weber, F.V. Kowalski, A.L. Schawlow: Appl. Opt. **18**, 1983 (1979)
10. D. Leibfried, F. Schmidt-Kaler, M. Weitz, T.W. Hänsch: Appl. Phys. B **56**, 65 (1983)
11. Z. Bay, G.G. Luther, J.A. White: Phys. Rev. Lett. **29**, 189 (1972)
12. R.G. DeVoe, R.G. Brewer: Phys. Rev. A **30**, 2827 (1984)
13. R.G. DeVoe, C. Fabre, K. Jungmann, J. Hoffnagle, R.G. Brewer: Phys. Rev. A **37**, 1802 (1988)
14. R.W.P. Drever, J.L. Hall, F.V. Kowalski, J. Hough, G.M. Ford, A.J. Munley, H.W. Ward: Appl. Phys. B **31**, 97 (1983)
15. I. Steiner, V. Enders, F. Elsner, W. Neuhauser, P.E. Toschek, R. Blatt, J. Helmcke: Appl. Phys. B **49**, 251 (1989)
16. M. Born, E. Wolf: *Principles of Optics*, 6th edn. (Pergamon, New York 1980)
17. A. Schenzle, R.G. DeVoe, R.G. Brewer: Phys. Rev. A **25**, 2606 (1982)
18. W. Lichten: J. Opt. Soc. Am. B **2**, 1869 (1985)
    W. Lichten: J. Opt. Soc. Am. B **3**, 606 (1986)
19. P.W. Baumeister, F.A. Jenkins: J. Opt. Soc. Am. **47**, 57 (1957)
20. J. Cariou, P. Luc: *Atlas du Spectre d'Absorption de la Molécule de Tellure* (Laboratoire Aime-Cotton, CNRS II, Orsay, France 1980)